Imaging of the fluorescence spectrum of a single fluorescent molecule by prism-based spectroscopy

Yoshikazu Suzuki[a], Tomomi Tani[b], Kazuo Sutoh[a,*], Shinji Kamimura[a]

[a] *Department of Life Sciences, Graduate School of Arts and Sciences, University of Tokyo, Komaba 3-8-1, Meguro, Tokyo 153-8902, Japan*
[b] *The Tokyo Metropolitan Institute of Medical Science, Honkomagome 3-18-22, Bunkyo, Tokyo 113-8613, Japan*

Received 30 November 2001; revised 28 December 2001; accepted 3 January 2002

First published online 22 January 2002

Edited by Amy McGough

Abstract We have devised a novel method to visualize the fluorescence spectrum of a single fluorescent molecule using prism-based spectroscopy. Equiping a total internal reflection microscope with a newly designed wedge prism, we obtained a spectral image of a single rhodamine red molecule attached to an essential light chain of myosin. We also obtained a spectral image of single-pair fluorescence resonance energy transfer between rhodamine red and Cy5 in a double-labeled myosin motor domain. This method could become a useful tool to investigate the dynamic processes of biomolecules at the single-molecule level. © 2002 Published by Elsevier Science B.V. on behalf of the Federation of European Biochemical Societies.

Key words: Dispersion prism; Single-molecule spectral imaging; Single-pair fluorescence resonance energy transfer; Fluorescence microscopy

1. Introduction

Recent advances in single-molecule detection provide us valuable information on the functions and dynamics of biomolecules that is difficult to obtain from ensemble measurements. To visualize the behavior of individual biomolecules, such as protein, DNA, or RNA, it is necessary to attach a certain probe to the target molecule. One example of a probe is a microbead. By trapping a microbead attached to a single biomolecule with optical tweezers, the movements of a single molecular motor, such as myosin, kinesin, or dynein, have been successfully measured with the nanometer and millisecond resolution [1–4]. In addition, rotational motions of F1-ATPase or RNA polymerase have also been detected using conventional optical microscopy with high temporal and spatial resolution by observing the motion of a microbead [5,6].

A fluorescent molecule is also an excellent probe for the detection of individual macromolecules [7,8]. For single-molecule fluorescence spectroscopy, there are two major techniques to investigate the conformational dynamics of biomolecules. One is the polarization analysis of fluorescence emitted from a single fluorophore. Several techniques have been developed to detect changes of the polarization of fluorescence from a single fluorescent molecule [9–13]. Single-molecule polarization studies have shown that conformational dynamics or rotational motions of target biomolecules can be detected from changes of orientation of a single fluorophore. Fluorescence resonance energy transfer (FRET) is another useful application of fluorescent probes to investigate the dynamics of intramolecular conformational changes or intermolecular interactions of biomolecules at the single-molecule level [14–19]. Since the FRET technique relies on the distance-dependent resonance energy transfer between a donor fluorophore and an acceptor fluorophore, it is essential to detect simultaneously two different colors of fluorescence. For processes in which three or more different biomolecules are involved, such as ligand-induced conformational changes of macromolecules or intermolecular interactions of several proteins, it would be necessary to discriminate more than three different colors of fluorescence at a time.

In this report, we developed a novel but simple technique for imaging the fluorescence spectrum of a single fluorescent molecule. With this technique, we obtained a spectral image of the single-pair FRET between rhodamine red and Cy5 conjugated to myosin motor domain. This method opens the way to multicolor imaging at the single-molecule level.

2. Materials and methods

2.1. Instrumentation for the spectral imaging of single fluorescent molecules

Total internal reflection fluorescence microscopy (TIRFM) was used for visualizing individual fluorescent molecules immobilized on the surface of a quartz slide (Fig. 1A). TIRFM with an incident laser beam from the condenser side through a quartz block was installed on a conventional inverted microscope (IX-70, Olympus), as previously reported [20]. A 532-nm YAG laser (ADLAS) was used for illumination. Its linearly polarized light was at first introduced into a polarization beam splitter after being passed through a λ/2 wave plate. The light intensity was attenuated by rotating this λ/2 wave plate. Then, the circularly polarized beam, which was obtained by letting the beam through a λ/4 wave plate, was introduced into the quartz block for total internal reflection. The gap between the quartz slide and the quartz block was filled with pure glycerol. The excitation beam was reflected at the interface between a quartz slide and sample solution to produce an evanescent field. A 100× objective (UPlanApo, 0.5–1.35 variable N.A., Olympus) was used for observations. A wide range bandpass barrier filter (HQ545lp, 545–770 nm, Chroma) was used to reject scattering light and background luminescence.

The fluorescence spectrum was visualized with a custom-made prism (Sigma Optics) inserted between the objective and intermediate magnifying lens of the microscope. We made the prism by gluing together two wedge elements made of different glass materials (BK7 and SF6), as shown in Fig. 1B. The angle and thickness of the wedge

*Corresponding author. Fax: (81)-3-5454 6751.
E-mail address: sutoh@bio.c.u-tokyo.ac.jp (K. Sutoh).

Abbreviations: FRET, fluorescence resonance energy transfer; TIRFM, total internal reflection fluorescence microscopy; ELC, essential light chain of myosin; TEAB, triethylamine bicarbonate buffer; EDC, 1-ethyl-3-(3-dimethylaminopropyl)carbodiimide

0014-5793/02/$22.00 © 2002 Published by Elsevier Science B.V. on behalf of the Federation of European Biochemical Societies.
PII: S0014-5793(02)02269-X

elements were designed so as to obtain appropriate dispersion of fluorescence light on the image plane without deflection of the main optical axis (green light). The images were captured with a cooled CCD video camera (Dage MTI) coupled to an image intensifier (VS4-1845, Video Scope International) and recorded on videotape after digitally processing with an image analyzer (Argus-50, Hamamatsu Photonics). The light intensity along the spectral image of single fluorescent molecules was determined with 8-bit resolution using custom-made software (Hamamatsu Photonics) installed in a personal computer (Epson). To record colored images of fluorescent microbeads, a color digital CCD camera (COOLPIX, Nikon) was used instead of the image intensifier and the cooled CCD camera.

2.2. Sample preparation

For the spectral imaging of a single fluorescent molecule, a recombinant essential light chain (ELC, 150 amino acids) of *Dictyostelium* myosin II labeled with a rhodamine red maleimide (Molecular Probes) was used. Rhodamine red has an absorption peak at 570 nm and an emission peak at 590 nm. Two endogenous cysteines (C11, C31) were replaced to alanine while the serine 38 was replaced to cysteine by site-directed mutagenesis for the labeling with rhodamine red maleimide. A hexahistidine-tag (His-tag) was attached to the N-terminus of the recombinant ELC gene to facilitate protein purification.

For single-pair FRET experiments, we used a recombinant *Dictyostelium* myosin heavy chain as well as the recombinant ELC. A motor domain of the *Dictyostelium* myosin II heavy chain (residues 1–793) with one IQ motif was constructed. Because C678 in the heavy chain is the most conserved cysteine residue and is thought to be reactive (called SH2 cysteine), it was replaced to serine by site-directed mutagenesis. It has been demonstrated that this cysteine-to-serine mutation does not significantly affect its ATPase and motility activities [21]. Then, a new cysteine residue was introduced at serine 54 by site-directed mutagenesis for the labeling with Cy5-maleimide. Cy5 has an absorption peak at 640 nm and an emission peak at 670 nm. His-tag was attached to the C-terminus of the recombinant motor domain to facilitate protein purification. Expression and purification were performed as previously described [22]. The procedures of protein labeling and reconstruction of the double-labeled motor domain will be described in detail elsewhere.

2.3. Synthesis of Cy5-maleimide

Cy5-maleimide was prepared as follows. ~2 μmol of Cy5-succinimidyl ester (Amersham Pharmacia) was reacted with a 20-fold molar excess of ethylenediamine in 50 μl of 0.5 M hydrogen bicarbonate, pH 8.5, at 25°C for 2 h. The reaction mixture was loaded on a MonoQ column (Pharmacia) equilibrated with a 10 mM TEAB (triethylamine bicarbonate) buffer, pH 8.3. After several washes with the equilibration buffer, Cy5-NH_2 was eluted by a linear gradient of 0.01–0.6 M TEAB, pH 8.3. The fractions of Cy5-NH_2 were collected, dried up by a rotary evaporator, and stored at −20°C if necessary. Next, the Cy5-NH_2 was reacted with excess *N*-methoxycarbonyl maleimide in 1.0 M TEAB, pH 8.3, at 0°C for ~2 h. The reaction mixture was applied to a MonoQ column equilibrated with a 10 mM triethanolamine–HCl buffer, pH 7.6. Cy5-maleimide was eluted with 0.5 M NaCl and used immediately to label proteins.

2.4. Protein immobilization on a quartz slide

Immobilization of proteins on the surface of a quartz slide was performed in a flow cell constructed by a quartz slide, a coverslip, and two sheets of thin waterproof paper as spacers. First, 5–20 mg/ml of BSA (bovine serum albumin) in deionized water was infused into the flow cell and kept there for 5 min. After several washes with 100 μl of a cross-linking buffer (0.1 M triethanolamine–HCl, pH 7.6), 100-fold diluted monoclonal anti-6×His antibodies (Clontech) and 0.1 M EDC (1-ethyl-3-(3-dimethylaminopropyl)carbodiimide) in the cross-linking buffer were infused and incubated for 5 min to form cross-links between the surface-coating BSA and the antibodies. The flow cell was then washed with 100 μl of 10 mM glycine solution several times to block unreacted EDC molecules. After 5 min incubation with the blocking buffer, the flow cell was washed several times with an assay buffer consisting of 20 mM MOPS, pH 7.4, 50 mM KCl, and 4 mM $MgCl_2$. Then, 20–200 nM of the labeled protein diluted with the assay buffer was introduced in the cell. The cell was washed more than 10 times with 100 μl of the assay buffer. Two sheets of spacers were removed before microscopic observations. All of the procedures described above were performed at room temperature.

3. Results

3.1. Spectral imaging of a fluorescent microbead using the dispersion prism

In order to test the performance of the dispersion prism designed in the present study, we first observed a fluorescent microbead (F-8784, diameter is 0.02 μm, Molecular Probes) placed on a quartz slide (Fig. 1C,D). Without the dispersion prism, the microbeads were observed as small orange spots (Fig. 1C). Inserting the dispersion prism into the optical path of the microscope, fluorescent light from the microbead was dispersed in the image plane, as shown in Fig. 1D. Since the fluorescence of the microbead contains a wide range of visible light, we could clearly distinguish several components of the fluorescence, e.g. green, yellow, and red bands in the spectral image of the microbead.

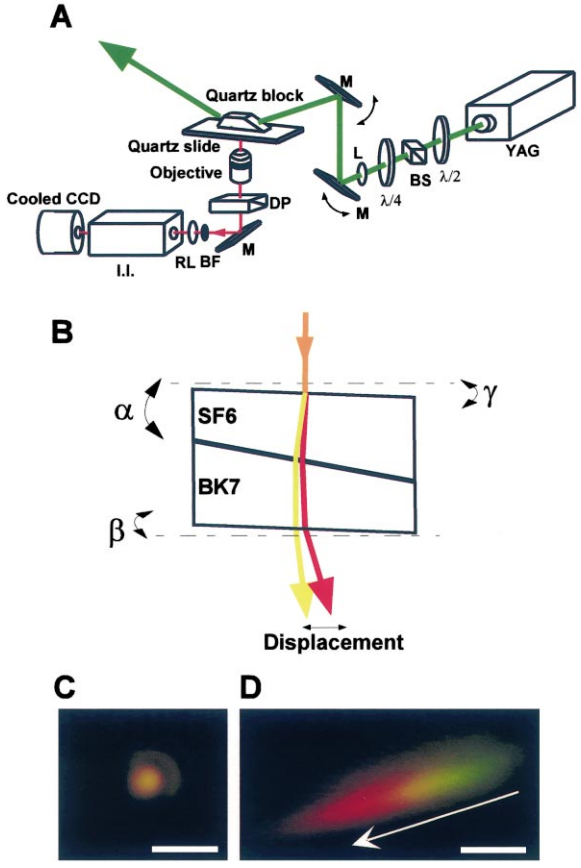

Fig. 1. Optical setup for spectral imaging of single fluorescent molecules. A: Schematic drawing of the total internal reflection microscope. A dispersion prism for spectroscopy was inserted immediately under an objective lens. λ/2 and λ/4, half- and quarter-wave plate, respectively; BS, polarizing beam splitter; M, reflection mirror; L, lens; DP, dispersion prism; BF, barrier filter; RL, relay lens. B: Schematic drawing of the dispersion prism. Two wedge prisms made of SF6 and BK7 were stuck to each other. The size of the dispersion prism was designed as 25 mm×25 mm×8.1 mm. $\alpha = 9.0°$, $\beta = 2.84°$, $\gamma = 2.17°$. C: A color image of a fluorescent microbead observed without the dispersion prism. Scale bar = 1 μm. D: A color spectral image of a fluorescent microbead observed with the dispersion prism. The arrow indicates the direction to the longer wavelength in the spectral image. Scale bar = 1 μm.

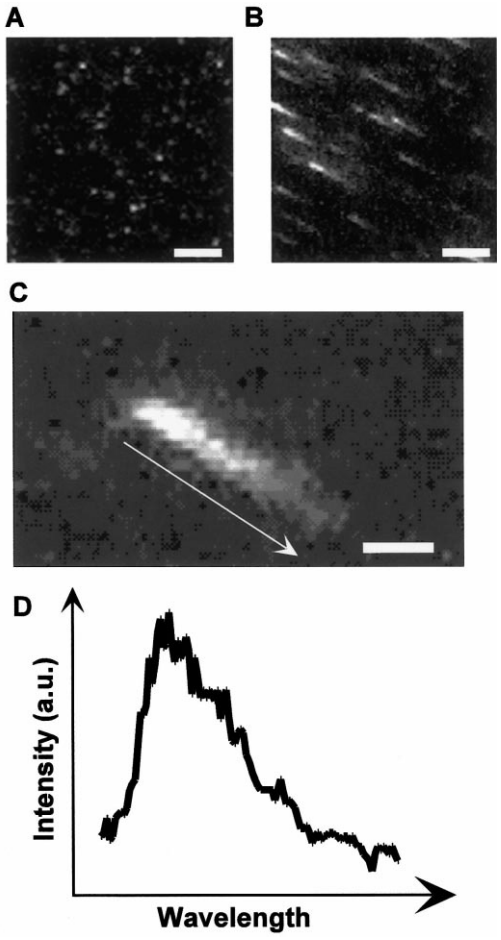

Fig. 2. Spectral imaging of individual rhodamine red molecules immobilized on a quartz slide. A and B: Images of individual rhodamine red molecules conjugated to ELC with (B) and without (A) the dispersion prism. Each image was obtained by averaging eight video frames. Scale bar = 5 μm. C: A typical fluorescence spectral image of a single rhodamine red molecule. This image was obtained by averaging 16 video frames. The arrow indicates the direction to the longer wavelength. Scale bar = 1 μm. D: A fluorescence spectrum of a single rhodamine red molecule. This spectrum was obtained by plotting the fluorescence intensity pixel by pixel along the spectral image shown in C.

3.2. Spectral imaging of a single rhodamine red molecule attached to a single protein

The ELC labeled with rhodamine red was immobilized on a quartz slide and observed by TIRFM. When observed without the dispersion prism, the fluorescence of the individual rhodamine red molecules attached to ELC was observed as a fluorescence spot (Fig. 2A). During excitation, almost all of the fluorescence spots disappeared in one step by photobleaching (data not shown). The observation indicates that each fluorescence spot corresponded to a single rhodamine red molecule, since the emission from a single fluorophore is photobleached in one step [14].

Fig. 2B shows images of individual rhodamine red-labeled ELCs observed with the dispersion prism. Here, the fluorescence from individual rhodamine red molecules was dispersed by the dispersion prism, resulting in comet-shaped streaks. These streaks correspond to each spectral feature of single rhodamine red molecules. Fig. 2C shows a typical example of images. When the fluorescence intensity was quantified pixel by pixel, the spectral image was converted into a single-molecule fluorescence spectrum, as shown in Fig. 2D. It should be noted that the shapes of observed fluorescence spectra were not exactly the same as those obtained for ensemble samples by a spectrofluorometer since the refractive index of light is not linearly dependent on the wavelength.

3.3. Observation of single-pair FRET using the dispersion prism

Individual double-labeled myosin motor domains immobilized on a quartz slide were observed through the dispersion prism (Fig. 3A). A typical spectral image of the single-pair FRET between rhodamine red and Cy5 in the single myosin motor domain is shown in Fig. 3B. Since both the leakage of rhodamine red fluorescence in the Cy5 region and the emission of Cy5 directly excited with the 532-nm light are negligible, it is most likely that the strong emission of Cy5 is due to

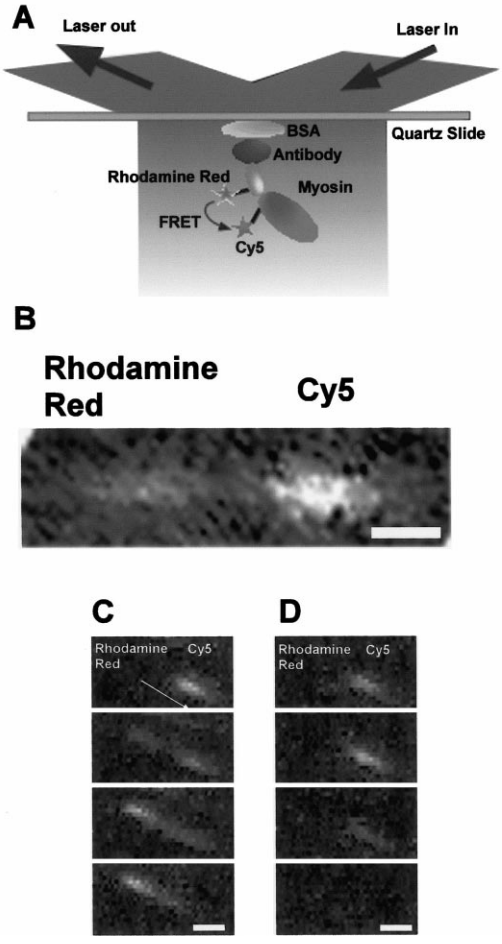

Fig. 3. Single-pair FRET in a reconstructed double-labeled myosin motor domain. A: Schematic drawing of the single-pair FRET experiment. The ELC and heavy chain of the myosin motor domain were labeled with rhodamine red (donor) and Cy5 (acceptor), respectively. B: A typical spectral image of the single-pair FRET observed with a broadband barrier filter (545–770 nm). Emission of rhodamine red and Cy5 was separated well by the dispersion prism. The strong fluorescence of Cy5 is due to FRET between the two fluorescent dyes. Scale bar = 1 μm. C and D: Time courses of photobleaching events in the single-pair FRET. C: The acceptor (Cy5) was photobleached first. D: The donor (rhodamine red) was photobleached first. Images were obtained by averaging 16 video frames, and the averaged images were vertically placed according to the duration of the laser illumination. The arrow indicates the direction to the longer wavelength. Scale bar = 1 μm.

FRET from a single rhodamine red molecule to a single Cy5 molecule in the motor domain. The notion was supported by the analysis of photobleaching events. When the acceptor (Cy5) was photobleached first, the fluorescence intensity of the donor (rhodamine red) was increased with the concomitant disappearance of Cy5 fluorescence (Fig. 3C). This anti-correlation of donor–acceptor fluorescence is the direct evidence for the single-pair FRET [14]. Consistent with the observation, the emission of the acceptor disappeared simultaneously when the donor was photobleached (Fig. 3D).

4. Discussion

We have devised a method for single-molecule fluorescence spectroscopy using a newly designed dispersion prism incorporated into TIRFM. By this method, we succeeded to visualize the spectrum of a single fluorescent molecule. Since the dispersion prism consists of two wedge elements with different refractive indices glued together, the light passing through the prism was dispersed according to the wavelength. The angles of the two wedge elements were carefully chosen to reduce the deflection angle of light passing through the prism. Therefore, the specimen image can be easily compared before and after the insertion of a prism into the optics that makes fluorescence images of streaked lines in place of fluorescent spots (Fig. 2A,B). From the recorded streak images we can analyze spectra of each fluorescent dye.

For the similar analysis of fluorescence spectrum, another technique has been reported so far using dispersion by a conventional prism that is placed in the optical pass of the microscope [23]. Although this method has provided better accuracy of spectrum, a difficult point is that it cannot be easily available for usual fluorescence microscopy since quite a big modification of the microscope optics is required. In contrast, the present technique with a prism consisting of two wedge elements could be easily applied to any kind of microscope system by simply placing a similar prism between the objective and the ocular lenses. Although the temporal resolution of data presented in this report is still low ($\sim$0.5 s) because of the frame-averaging procedure for getting images of good signal-to-noise ratio, a higher resolution will be achieved using a high-speed digital CCD camera of low background noise.

We also succeeded to visualize a single-pair FRET as a spectral image using the double-labeled myosin motor domain. The strong emission of Cy5 and weak emission of rhodamine red observed in the single-pair FRET indicate that the excited energy of the donor was almost fully transferred to the acceptor due to the close proximity of the two fluorophores. In the crystal structure of the myosin motor domain, the distance between S54 of a heavy chain and S38 of ELC is about 37 Å in the absence of nucleotides [24]. The calculated critical distance (R_0), where FRET efficiency is 50%, between rhodamine red and Cy5, is estimated as 52 Å, which is much longer than the distance between the donor and the acceptor expected from the crystal structure. Therefore, it is reasonable that the Cy5 emission was much stronger than the rhodamine red emission in the spectral image of a single-pair FRET. It should be noted here that the apparently narrower spectral width of Cy5 than that of rhodamine red (Fig. 3B) is due to the fact that the refractive index becomes smaller as the wavelength becomes longer.

Several single-molecule spectroscopy analyses using a pinhole filter with gratings have previously been reported [25,26]. They achieved a high spectral resolution, demonstrating the existence of a time-dependent spectral shift accompanied by changes in the environments surrounding the fluorophore with an accuracy of several nanometers. However, only the spectrum of a single chosen molecule was analyzed with the grating-based method. On the contrary, the present method using prism-based single-molecule spectroscopy can treat many spectral data of single fluorescent molecules at the same time although with a lower spectral resolution. This allows us to quickly characterize the spectral features of many molecules at the same time. Furthermore, it must also be noticed that prism-based spectroscopy can be useful for the detection of a spectrum composed of fluorescence from more than two different dyes, which is difficult to detect with conventional techniques of fluorescence microscopy. Therefore, this technique could be a very powerful tool to investigate intermolecular interactions and conformational changes induced by ligand binding, in which several different molecules are simultaneously involved.

Acknowledgements: We thank Dr. Yanagida (Osaka University) and his colleagues for their participation in helpful discussions on techniques of single-molecule imaging. We also thank Dr. Spudich (Stanford University) and Dr. Chisholm (Northwestern University) for providing the myosin heavy chain and ELC genes, respectively. This work was supported by Grants-in-Aid for Scientific Research from the Ministry of Education (K.S. and S.K.) and from the Japan Society for the Promotion of Science for Young Scientists (Y.S.).

References

[1] Finer, J.T., Simmons, R.M. and Spudich, J.A. (1994) Nature 368, 113–119.
[2] Molloy, J.E., Burns, J.E., Kendrick, J.J., Tregear, R.T. and White, D.C. (1995) Nature 378, 209–212.
[3] Svoboda, K., Schmidt, C.F., Schnapp, B.J. and Block, S.M. (1993) Nature 365, 721–727.
[4] Sakakibara, H., Kojima, H., Sakai, Y., Katayama, E. and Oiwa, K. (1999) Nature 400, 586–590.
[5] Yasuda, R., Noji, H., Yoshida, M., Kinosita Jr., K. and Itoh, H. (2001) Nature 410, 898–904.
[6] Harada, Y., Ohara, O., Takatsuki, A., Itoh, H., Shimamoto, N. and Kinosita Jr., K. (2001) Nature 409, 113–115.
[7] Weiss, S. (1999) Science 283, 1676–1683.
[8] Weiss, S. (2000) Nat. Struct. Biol. 7, 724–729.
[9] Sosa, H., Peterman, E.J., Moerner, W.E. and Goldstein, L.S. (2001) Nat. Struct. Biol. 8, 540–544.
[10] Adachi, K., Yasuda, R., Noji, H., Itoh, H., Harada, Y., Yoshida, M. and Kinosita Jr., K. (2000) Proc. Natl. Acad. Sci. USA 97, 7243–7247.
[11] Warshaw, D.M. et al. (1998) Proc. Natl. Acad. Sci. USA 95, 8034–8039.
[12] Sase, I., Miyata, H., Ishiwata, S. and Kinosita Jr., K. (1997) Proc. Natl. Acad. Sci. USA 94, 5646–5650.
[13] Harms, G.S., Sonnleitner, M., Schutz, G.J., Gruber, H.J. and Schmidt, T. (1999) Biophys. J. 77, 2864–2870.
[14] Ha, T., Enderle, T., Ogletree, D.F., Chemla, D.S., Selvin, P.R. and Weiss, S. (1996) Proc. Natl. Acad. Sci. USA 93, 6264–6268.
[15] Deniz, A.A., Dahan, M., Grunwell, J.R., Ha, T., Faulhaber, A.E., Chemla, D.S., Weiss, S. and Schultz, P.G. (1999) Proc. Natl. Acad. Sci. USA 96, 3670–3675.
[16] Zhuang, X., Bartley, L.E., Babcock, H.P., Russell, R., Ha, T., Herschlag, D. and Chu, S. (2000) Science 288, 2048–2051.
[17] Ha, T., Ting, A.Y., Liang, J., Caldwell, W.B., Deniz, A.A., Chemla, D.S., Schultz, P.G. and Weiss, S. (1999) Proc. Natl. Acad. Sci. USA 96, 893–898.
[18] Ha, T., Zhuang, X., Kim, H.D., Orr, J.W., Williamson, J.R. and Chu, S. (1999) Proc. Natl. Acad. Sci. USA 96, 9077–9082.

[19] Talaga, D.S., Lau, W.L., Roder, H., Tang, J., Jia, Y., DeGrado, W.F. and Hochstrasser, R.M. (2000) Proc. Natl. Acad. Sci. USA 97, 13021–13026.
[20] Funatsu, T., Harada, Y., Tokunaga, M., Saito, K. and Yanagida, T. (1995) Nature 374, 555–559.
[21] Suzuki, Y., Ohkura, R., Sugiura, S., Yasuda, R., Kinoshita, K.J., Tanokura, M. and Sutoh, K. (1997) Biochem. Biophys. Res. Commun. 234, 701–706.
[22] Sasaki, N., Shimada, T. and Sutoh, K. (1998) J. Biol. Chem. 273, 20334–20340.
[23] Lacoste, T.D., Michalet, X., Pinaud, F., Chemla, D.S., Alivisatos, A.P. and Weiss, S. (2000) Proc. Natl. Acad. Sci. USA 97, 9461–9466.
[24] Rayment, I. et al. (1993) Science 261, 50–58.
[25] Wazawa, T., Ishii, Y., Funatsu, T. and Yanagida, T. (2000) Biophys. J. 78, 1561–1569.
[26] Jung, G., Wiehler, J., Göhde, W., Tittel, J., Basché, Th., Steipe, B. and Bräuchle, C. (1998) Bioimaging 6, 54–61.